GEOPHYSICS, VOL. 58, NO. 2 (FEBRUARY 1993); P. 215-226, 17 FIGS.

Three-dimensional magnetotelluric modeling using difference equations-Theory and comparisons to integral equation solutions

Randall L. Mackie*, Theodore R. Madden*, and Philip E. Wannamaker‡

ABSTRACT

We have developed an algorithm for computing the magnetotelluric response of three-dimensional (3-D) earth models. It is a difference equation algorithm that is based on the integral forms of Maxwell's equations rather than the differential forms. This formulation does not require approximating derivatives of earth properties or electromagnetic fields, as happens when using the second-order vector diffusion equation. Rather, one must determine how averages are to be computed. Side boundary values for the H fields are obtained from putting two-dimensional (2-D) slices of the model into a larger-scale 2-D model and solving for the fields at the 3-D boundary positions. To solve the 3-D system of equations, we propagate an impedance matrix, which relates all the horizontal E fields in a layer to all the horizontal H fields in that same layer, up through the earth model. Applying a plane-wave source condition and the side boundary H field values allows us to solve for the unknown fields within the model. The results of our method compare favorably with results from previously published integral equation solutions.

INTRODUCTION

In recent years, a lot of effort has gone into developing three-dimensional (3-D) magnetotelluric modeling algorithms. Much of this work has concentrated on the integral equation approach (e.g., Hohmann, 1975; Weidelt, 1975; Wannamaker et al., 1984a; San Filipo and Hohmann, 1985; Wannamaker, 1991), and it has become the standard against which other methods are measured. Integral equation solutions are computationally quick when there are only a few inhomogeneous bodies in an otherwise layered earth. As the complexity of the model increases, however, so also does the computation time. On the other hand, finite-difference and finite-element algorithms (e.g., Jones and Pascoe, 1972; Reddy et al., 1977) are better suited to model arbitrarily complex geometries, but their use has not been as widespread since they lead to large systems of equations to be solved even for simple models. Recent advances in iterative relaxation techniques (Sarkar, 199 1) and continuously increasing computing power will, in the future, allow for finite-difference and finite-element modeling of more complicated' 3-D earth models than at the present time.

In developing an algorithm for 3-D magnetotelluric modeling, we were motivated by the desire to be able to model arbitrarily complex media, which is especially important when inversions are to be done. This led us to use differential methods over integral methods, and within the class of differential methods, finite differences are simpler to implement than finite elements. The earliest 3-D finite-difference magnetotelluric modeling algorithms were developed by Jones and Pascoe (1972) and Lines and Jones (1973a). Their algorithms solved the second-order vector diffusion equation in E over a 3-D mesh for simple models using a Gauss-Seidel iterative scheme (Jones, 1974). That work was also modified to consider nonuniform source fields (Hibbs and Jones, 1976). Later, Zhdanov et al. (1982) explored the application of asymptotic boundary conditions to the finite-difference scheme, although no numerical examples were shown for the 3-D case. Applications to time-domain solutions were presented by Adhidjaja and Hohmann (1989), who developed a finite-difference algorithm for computing the transient electromagnetic response of a 3-D body using a Du Fort-Frankel differencing scheme. Their results were limited to only small models and were not in good agreement with integral equation solutions, possibly due to rapidly varying source fields, grid inaccuracies, and using a combination of numerical and analytic computations for the source terms. Finally, progress in 3-D finite-difference modeling is being made independently by other research groups, although their results have not as yet been formally published.

Manuscript received by the Editor October 30, 1991; revised manuscript received July 17, 1992.
*Massachusetts Institute of Technology, Department of Earth, Atmospheric and, Planetary Sciences, Room 54-616, Cambridge, MA 02139.
‡University of Utah Research Institute, 391-C Chipeta Way, Salt Lake City, UT 84108.

Xinghua et al. (1991) have developed a new 3-D finite-difference modeling algorithm that solves directly for the three magnetic components and incorporates a thin sheet above a general 2-D or 3-D structure, and (Smith, J. T., 1992, personal communication) has developed an iterative 3-D finite difference algorithm on a staggered grid that appears to be quick and accurate.

It also is important to point out that 3-D finite difference solutions to Maxwell's equations have also been developed quite extensively in the electrical engineering domain, although not necessarily applied to electromagnetic induction in earth models. The earliest such work for general 3-D models was done by Yee (1966) who derived a staggered grid finite-difference, time-domain algorithm for computing the electromagnetic scattering off perfectly conducting surfaces. (It turns out that our 3-D modeling algorithm is actually a frequency-domain equivalent of Yee's (1966) algorithm, although our derivation is slightly different from his.) More recently, Taflove (1988) and Morgan (1990) review the current generation of finite-difference electromagnetic scattering algorithms used in the electrical engineering domain for a broad range of applications.

Our finite-difference modeling algorithm differs from much of the previous work in that we start from the integral forms of Maxwell's equations rather than the differential forms. This formulation does not involve differentiation, although it leads to the same difference equations as if one approximated the first-order differential Maxwell equations. Finite-difference schemes based on the differential forms of Maxwell's equations can be interpreted as approximations to the pointwise derivatives using numerical differences (Taflove and Umashankar, 1990). On the other hand, finite-difference schemes based on the integral forms of Maxwell's equations provide one with a simple geometrical understanding of the coupling between Ampere's Law and Faraday's Law (Taflove and Umashankar, 1990), and the difference equations result naturally from the application of the contour integrals to flat surfaces defined by a regular discretization of space. The main issues one faces, however, are involved with defining averages, which seems to be a more natural approach to a discretized approximation than trying to define finite-difference approximations to derivatives. It turns out that averages are even used in dealing with finite-difference approximations to derivatives of earth conductivities, as arises when discretizing the second-order differential equations (Brewitt-Taylor and Weaver, 1976). Once averages are defined, it is a fairly simple matter to solve the first-order equations using an impedance propagator technique, although iterative relaxation techniques can also be used to decrease the computation time and memory requirements for a solution (Jones, 1974; Mackie, 1991; Sarkar, 1991).

DIFFERENCE EQUATIONS

At the low frequencies involved in magnetotelluric exploration, conduction currents dominate over displacement currents. Therefore, if displacement currents are ignored and an $e^{-i\omega t}$ time dependence is assumed, then the integral forms of Maxwell's equations in mks units are given by:

$$\oint \mathbf{H} \cdot d\mathbf{l} = \int\int \mathbf{J} \cdot d\mathbf{S} = \int\int \sigma\mathbf{E} \cdot d\mathbf{S} \qquad (1a)$$

$$\oint \mathbf{E} \cdot d\mathbf{l} = \int\int i\mu\omega\mathbf{H} \cdot d\mathbf{S}, \qquad (1b)$$

where in general, σ and μ are tensor quantities (Stratton, 1941). It is straightforward to define a geometry so that either equation (la) or (lb) is exactly satisfied. For example, **H** defined as the average along block edges and $\sigma\mathbf{E}$ defined as the average across the block surfaces would lead to difference equations that would be exact for equation (la). However, this geometry would be inconsistent for equation (lb) since in that equation E is defined as the average along a contour and H is defined as the average across the surface outlined by the contours. This difference in geometry is what makes the difference equations an approximation. We would like to point out, however, that all difference equation solutions involve approximations whether it is approximating the integral equations or approximating derivatives of the fields and earth properties. These are first-order difference equations that have the advantage that one avoids having to deal with derivatives of earth properties, as happens when the second-order system of equations is discretized.

We divide the earth model into rectangular blocks of arbitrary dimensions with the H field defined along block edges, and the J and E fields defined along the normals to the block faces, as shown in Figure 1. This is equivalent to the geometry for a finite-difference scheme on a staggered grid developed by Yee (1966). (One could alternatively define E along the block edges and H along the normals to the block faces.) Since the H field components surround the block faces, equation (la) can be used to derive the total current flow across the face. The J fields are continuous across block interfaces, but the associated E fields will suffer discontinuities if adjoining blocks have differing conductivities. Discontinuities in the E field do not pose any problems since these equations involve integrations rather than differentiations. The contours for equation (lb) are taken around flat surfaces centered on the block edges and outlined by the normals to the block faces, as shown in Figure 1.

One can transform any unequally gridded earth to an equally gridded earth by making the appropriate transformations in the conductivity, permeability, and field values (Madden and Mackie, 1989). This is useful for two reasons. First, an equally gridded mesh results in an operator for the difference equations that is symmetric, which would generally not be the case if the spacing were variable. This is important when solving the problem by conjugate direction relaxation techniques that assume symmetric operators. Second, taking averages is simplified after transforming to equally spaced grids since the proper weighting of the fields and earth properties is taken into account by the scaling factors.

If the transformed parameters are denoted with an apostrophe, then the scaling factors for the transformation are

$$C_x = \frac{\Delta x}{\Delta x'} \quad C_y = \frac{\Delta y}{\Delta y'} \quad C_z = \frac{\Delta z}{\Delta z'}, \qquad (2)$$

and the transformed conductivity and permeability tensors are

$$\sigma' = \begin{bmatrix} \sigma \dfrac{C_y C_z}{C_x} & 0 & 0 \\ 0 & \sigma \dfrac{C_x C_z}{C_y} & 0 \\ 0 & 0 & \sigma \dfrac{C_x C_y}{C_z} \end{bmatrix} \quad (3)$$

$$\mu' = \begin{bmatrix} \mu \dfrac{C_y C_z}{C_x} & 0 & 0 \\ 0 & \mu \dfrac{C_x C_z}{C_y} & 0 \\ 0 & 0 & \mu \dfrac{C_x C_y}{C_z} \end{bmatrix} \quad (4)$$

For our application, we assume isotropic conductivity, but the generalization to anisotropic media is straightforward. We also assume that $\mu = \mu_0 = 4\pi \times 10^{-7}$ H/m everywhere. The transformed E, H, and J fields are defined as

$$E'_x = C_x E_x \quad E'_y = C_y E_y \quad E'_z = C_z E_z \quad (5a)$$

$$H'_x = C_x H_x \quad H'_y = C_y H_y \quad H'_z = C_z H_z \quad (5b)$$

$$J'_x = C_y C_z J_x \quad J'_y = C_x C_z J_y \quad J'_z = C_x C_y J_z . \quad (5c)$$

Under these transformations, equations (la) and (lb) remain invariant, so that solving the transformed system is equivalent to solving the original or untransformed system. Throughout the remainder of this paper it will be assumed that we are dealing with the transformed variables, and the apostrophes will be dropped. Furthermore, to ensure symmetry, it is required that $\Delta x' = \Delta y' = \Delta z' = L$.

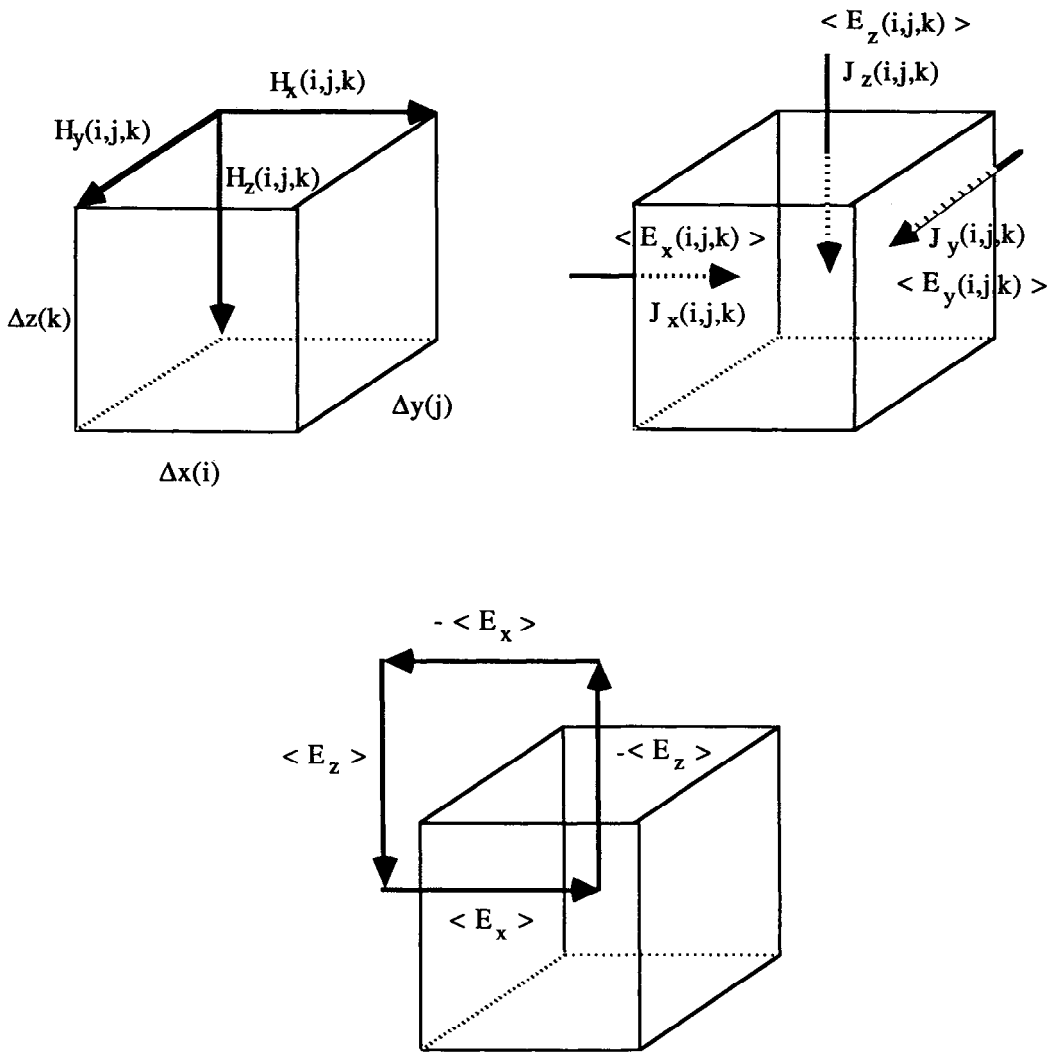

FIG. 1. The difference equation geometry based on the integral forms of Maxwell's equations. The earth model is divided into rectangular blocks of arbitrary dimensions. Each block has resistivity $\rho(i, j, k)$ and magnetic permeability μ_0. The H fields are defined as averages along block edges, and the J and E fields are defined as averages along the normals to the block faces. The contours for equation (1a) are taken along the edges of the block faces. The contours for equation (1b) are taken around flat surfaces centered on the block edges and outlined by the normals to the block faces and are shown at the bottom of the figure.

With this formulation and the geometry shown in Figure 1, the x, y, and z components of equation (1a) are

$$\begin{aligned}
&\{[H_z(i, j+1, k) - H_z(i, j, k)] - [H_y(i, j, k+1) \\
&\qquad - H_y(i, j, k)]\}L = J_x(i, j, k)L^2, \\
&\{[H_x(i, j, k+1) - H_x(i, j, k)] - [H_z(i+1, j, k) \\
&\qquad - H_z(i, j, k)]\}L = J_y(i, j, k)L^2, \\
&\{[H_y(i+1, j, k) - H_y(i, j, k)] - [H_x(i, j+1, k) \\
&\qquad - H_x(i, j, k)]\}L = J_z(i, j, k)L^2.
\end{aligned} \tag{6}$$

The J fields are continuous, but the E fields suffer discontinuities when adjoining blocks have differing conductivities. It is natural, therefore, to define the E fields along the block face normals as the average of the E fields on either side of the block face which, since J is continuous, can be written as

$$\begin{aligned}
E_x(i, j, k) &= \frac{[\rho_{xx}(i, j, k) + \rho_{xx}(i-1, j, k)]}{2} J_x(i, j, k), \\
E_y(i, j, k) &= \frac{[\rho_{yy}(i, j, k) + \rho_{yy}(i, j-1, k)]}{2} J_y(i, j, k), \\
E_z(i, j, k) &= \frac{[\rho_{zz}(i, j, k) + \rho_{zz}(i, j, k-1)]}{2} J_z(i, j, k).
\end{aligned} \tag{7}$$

The resistivities are subscripted because the transformed resistivity tensor is anisotropic with principle directions x, y, and z, even though the actual resistivities are isotropic, as in equation (3). This likewise applies to the magnetic permeabilities. The components of equation (lb) are given by

$$\begin{aligned}
&\{[E_z(i, j, k) - E_z(i, j-1, k)] - [E_y(i, j, k) \\
&\qquad - E_y(i, j, k-1)]\}L = i\omega\langle\mu_{xx}\rangle H_x(i, j, k)L^2 \\
&\{[E_x(i, j, k) - E_x(i, j, k-1)] - [E_z(i, j, k) \\
&\qquad - E_z(i-1, j, k)]\}L = i\omega\langle\mu_{yy}\rangle H_y(i, j, k)L^2, \\
&\{[E_y(i, j, k) - E_y(i-1, j, k)] - [E_x(i, j, k) \\
&\qquad - E_x(i, j-1, k)]\}L = i\omega\langle\mu_{zz}\rangle H_z(i, j, k)L^2.
\end{aligned} \tag{8}$$

where we define the average permeabilities as:

$$\begin{aligned}
\langle\mu_{xx}\rangle &= \frac{\mu_{xx}(i,j-1,k-1)+\mu_{xx}(i,j,k-1)+\mu_{xx}(i,j-1,k)+\mu_{xx}(i,j,k)}{4}, \\
\langle\mu_{yy}\rangle &= \frac{\mu_{yy}(i-1,j,k-1)+\mu_{yy}(i,j,k-1)+\mu_{yy}(i-1,j,k)+\mu_{yy}(i,j,k)}{4}, \\
\langle\mu_{zz}\rangle &= \frac{\mu_{zz}(i-1,j-1,k)+\mu_{zz}(i-1,j,k)+\mu_{zz}(i,j-1,k)+\mu_{zz}(i,j,k)}{4}.
\end{aligned} \tag{9}$$

One can solve the first-order system of equations, or one can algebraically eliminate either E or H to obtain a second-order system of equations. The direct solution technique described in this paper solves the first-order system of equations (after eliminating H_z and E_z). The E and H fields are output on the earth's surface at the top face center of each model block. Since the H fields are defined along block edges, the H fields in the center at the earth's surface (H_{xs} and H_{ys}) are simply taken to be the average of the adjacent H fields (here ks refers to the top, or surface, earth layer):

$$\begin{aligned}
H_{xs}(i, j) &= \frac{1}{2}[H_x(i, j, ks) + H_x(i, j+1, ks)] \\
H_{ys}(i, j) &= \frac{1}{2}[H_y(i, j, ks) + H_y(i+1, j, ks)].
\end{aligned} \tag{10}$$

Since the E fields in the model are defined as normals across the block faces, more care must be taken in computing the fields at the earth's surface. First, we compute the E fields in the top model block centers (E_{xc} and E_{yc}) using the average of the J fields across the corresponding block faces (e.g., $J_{xc}(i, j, ks) = [J_x(i, j, ks) + J_x(i-1, j, ks)]/2$). From equation (7), it then follows that

$$\begin{aligned}
E_{xc}(i, j) &= \frac{\rho(i, j, ks)}{\rho(i, j, ks) + \rho(i-1, j, ks)} E_x(i, j, ks) \\
&\quad + \frac{\rho(i, j, ks)}{\rho(i, j, ks) + \rho(i+1, j, ks)} E_x(i+1, j, ks) \\
E_{yc}(i, j) &= \frac{\rho(i, j, ks)}{\rho(i, j, ks) + \rho(i, j-1, ks)} E_y(i, j, ks) \\
&\quad + \frac{\rho(i, j, ks)}{\rho(i, j, ks) + \rho(i, j+1, ks)} E_y(i, j+1, ks).
\end{aligned} \tag{11}$$

Then, the E fields are continued up to the earth's surface using equation (8) modified to account for the different geometry and also setting $E_z = 0$, which is correct just under the surface because of the large resistivity contrast between the earth and the atmosphere.

BOUNDARY CONDITIONS, GRADING OF MODELS

Proper treatment of the model boundaries is important in calculating the magnetotelluric response of realistic 3-D models. One common approach is to assume that the model is periodic in the horizontal direction. This approach is used in Fourier methods (Park, 1983) and Rayleigh-FFT (fast-Fourier transform) methods (Jiracek et al., 1989), and it can also be used in difference equations. However, even if the boundaries are extended a considerable distance away from the local 3-D structure, there are still many situations where this would not be an accurate representation of the regional structure. This is because oftentimes, local magnetotelluric fields are biased by regional features far away from the local measurement site. The ocean-continent boundary is perhaps the most severe example of this (Ranganayaki and Madden, 1980).

In our modeling algorithm, we assign the tangential H fields on the boundaries of the 3-D model. This is in essence

assigning the regional current field a priori, both laterally and vertically. These boundary values come from a 2-D TM mode calculation where each vertical plane of the 3-D model is treated as the inner part of a larger-scale 2-D model. The values obtained at the positions corresponding to the boundaries of the 3-D model are used as the boundary values for the full 3-D calculations. This is not the most sophisticated method for assigning boundary values, but if the side boundaries are put far enough away from the 3-D inhomogeneity and the larger-scale 2-D models are similar for each 3-D slice, then the boundary values will be smoothly varying and the error in the solution will be reduced, but at the expense of the model being less realistic.

It is possible to extend the side boundaries to large distances without creating unmanageably large systems by grading the 3-D model in the horizontal directions (e.g., Lines and Jones, 1973b). Discretizing the model on a finer scale near regions of strong conductivity gradients allow us to obtain more accurate solutions. We can also grade the model in the vertical direction because: (1) the diffuse nature of electromagnetic waves in conducting media smears the information content with depth and (2) this allows us to use the same model for a wide range of frequencies without changing the vertical spacing, at least up to some high-frequency limit that is determined by the thickness and conductivity of the first layer. We found (Madden and Mackie, 1989) that geometrical grading factors of 2 in the vertical direction and factors of 3 in the horizontal directions gave results accurate to within 1 percent in amplitude and less than a degree in phase. These results applied to 1-D and 2-D geometries, but our own modeling experience has been that these results are probably valid for 3-D calculations.

Several graded air layers are added on top of the earth model to account for perturbations in the H fields from lateral current gradients. All of the H field perturbations are required to be damped out at the top of the air layers. These air layers extend far above the earth. All the results in this paper are from computations with the air layers extending to 75 km above the earth. We ran a test case for the model tested in this paper with the air layers extending to 150 km above the earth, but this did not result in any appreciable differences in the computed field values compared to those that had the air layers to 75 km above the earth. It is probably necessary, however, to extend the air layers to greater than 75 km for ocean-continent models since the height scale of the air layers is related to the width scale of the H field variations. At the bottom of the earth model, a 1-D impedance for a layered earth is used to relate the E field to the H field. Thus, it helps to have the bottom of the model below the resistivity lower crust, which acts to filter out shorter wavelength H field variations.

DIRECT SOLUTION: IMPEDANCE MATRIX FORMULATION

The system of equations resulting from the discretization of Maxwell's equation has a coefficient matrix that is large, sparse, and structured. Relaxation algorithms are one method for dealing with such systems. Sparse matrix inversion routines are another method that take advantage of the structure and sparsity of the matrix. However, we will use a Ricatti equation approach (Eckhardt , 1963), which propagates the impedance matrix from the bottom of the model to the surface. This reduces the size of the matrices to be inverted, but it also has the advantage that different models with the same lower layers can reuse the propagator results, which reduces the computations.

If E_z and H_z are eliminated from the discretized system of equations given earlier, then the horizontal E or H fields in one layer can be expressed in terms of the fields in that layer and the one below it. For example, since by equations (6) and (7), E_z is given by

$$E_z(i,j,k)=\frac{\rho_{zz}(i,j,k)+\rho_{zz}(i,j,k-1)}{2L}[H_y(i+1,j,k) - H_y(i,j,k) - H_x(i,j+1,k)+H_x(i,j,k)] \quad (12)$$

then E_x in the k - 1 layer, by virtue of equation (8), can be written in terms of the horizontal E and H fields in the kth layer directly below as

$$\begin{aligned} E_x(i,j,k-1) = {} & E_x(i,j,k) \\ & - \frac{\rho_{zz}(i,j,k)+\rho_{zz}(i,j,k-1)}{2L} \\ & \cdot [H_y(i+1,j,k) - H_y(i,j,k) \\ & + H_x(i,j,k)] + H_x(i,j,k) \\ & + \frac{\rho_{zz}(i-1,j,k)+\rho_{zz}(i-1,j,k-1)}{2L} \\ & \times [H_y(i,j,k) - H_y(i-1,j,k) \\ & - H_x(i-1,j+1,k) + H_x(i-1,j,k)] \\ & - i\omega\langle\mu_{yy}\rangle L H_y(i,j,k) \end{aligned} \quad (13)$$

Similar equations can also be written for E_y, H_x, and H_y. We can express these equations in a compact form as

$$\mathbf{E}_k = \underline{\mathbf{A}}_k\mathbf{H}_{k+1} + \mathbf{E}_{k+1} + \mathbf{a}_k, \quad (14)$$

$$\mathbf{H}_k = \underline{\mathbf{B}}_k\mathbf{E}_k + \mathbf{H}_{k+1}. \quad (15)$$

Here, $\mathbf{A}$ and $\underline{\mathbf{B}}$ are matrices that contain the coefficients in the equations for E_x, E_y, H_x, and H_y after E_z and H_z have been eliminated (such as equation (13) above), a is the vector that contains the contributions from the boundary tangential H fields (for example the terms in equation (13) that involve known boundary H field values), and E and H are the vectors of the unknown horizontal electric and magnetic fields, respectively.

If the E:H relationship is known at the k + 1 layer, then equations (14) and (15) can be combined to give

$$\begin{aligned} \mathbf{E}_k &= \underline{\mathbf{Z}}_k\mathbf{H}_k + \mathbf{z}_k, \\ \underline{\mathbf{Z}}_k &= [\underline{\mathbf{I}} + (\underline{\mathbf{A}}_k + \underline{\mathbf{Z}}_{k+1})\underline{\mathbf{B}}_k]^{-1}[\underline{\mathbf{A}}_k + \underline{\mathbf{Z}}_{k+1}], \\ \mathbf{z}_k &= [\underline{\mathbf{I}} + (\underline{\mathbf{A}}_k + \underline{\mathbf{Z}}_{k+1})\underline{\mathbf{B}}_k]^{-1}[\mathbf{a}_k + \mathbf{z}_{k+1}], \end{aligned} \quad (16)$$

and we can therefore propagate this up to the earth's surface. The starting relationship at the bottom of the model is taken as a 1-D plane-wave impedance for a layered media

representing the earth beneath the model. The impedance matrix $\underline{Z}$ does not grow exponentially coming up through the media as does the E and H fields, which makes the numerical propagation of the impedance matrix much more stable than trying to deal with the field values.

The source field for the magnetotelluric problem is a uniform current sheet at the earth's surface. Since it is uniform, the current sheet can be put anywhere above the earth's surface as long as we allow for the secondary outgoing fields above the current sheet. With the current sheet at the earth's surface, the tangential H field boundary terms in the air layers are zero, which means that the H field in the air is a secondary outgoing field that is equal to the H field due to the earth's conductivity structure minus the uniform field at the earth's surface.

As we did for the earth layers, it is very straightforward to derive a simple formula for propagating an air impedance matrix down to the earth's surface from the top of the air layers. The air is often taken to be an insulator in modeling algorithms, but our difference equations require a finite value for the resistivity of every model block [see equation (13)]. Therefore, we have set the resistivity of each air layer to IO" Ω m because this is still a large contrast to the earth's resistivity, but the value is not so large as to cause numerical problems. As before, we start at the top of the air layers with a plane-wave impedance appropriate for the atmosphere. The E:H relationship is continued layer by layer to the earth's surface using equations (14) and (15) except as just stated, the boundary terms are zero. This information can be written as

$$\begin{aligned} \mathbf{E}_{k+1} &= \underline{Z}_{k+1}\mathbf{H}_{k+1} \\ \underline{Z}_{k+1} &= \underline{Z}_k[\underline{I} - \underline{B}_k\underline{Z}_k]^{-1} - \underline{A}_k. \end{aligned} \tag{17}$$

We now have an earth impedance matrix, an air impedance matrix, and a uniform current sheet, all at the earth's surface. The E field is continuous across the current sheet, but there is a jump in the H field due to the current sheet. Therefore, we have the following relationships:

$$\begin{aligned} \mathbf{E}_{air} &= \underline{Z}_{air}\mathbf{H}_{air}, \\ \mathbf{E}_{earth} &= \underline{Z}_e\mathbf{H}_{earth} + \mathbf{z}_e \\ \mathbf{H}_{air} &= \mathbf{H}_{earth} - \mathbf{J}_{cs}, \end{aligned} \tag{18}$$

where J,, is the uniform current sheet at the earth's surface, $\mathbf{z}_e$ contains the effects of the side boundary values, $\mathbf{E}_{air}$ and $\mathbf{H}_{air}$ correspond to the unknown E and H fields just above the current sheet, and $\mathbf{E}_{e\,part\,h}$ and $\mathbf{H}_{earth}$ correspond to the unknown E and H fields just below the current sheet. Since E is continuous across the current sheet, we can write:

$$\mathbf{H}_{earth} = [\underline{I} - \underline{Y}_{air}\underline{Z}_e]^{-1}[J_{cs} + \underline{Y}_{air}\mathbf{z}_e]. \tag{19}$$

Once the H fields at the earth's surface are known, then the E fields at the surface can be determined as well as the E and H fields everywhere in the model using equations (14) and (IS). Thus, solving the 3-D model has been reduced to solving the EM interactions at each layer in the model rather than solving the EM interactions in the 3-D model as a whole at one time. This algorithm has the advantage ot directly solving the 3-D MT equations by doing several smaller matrix inversions rather than one large matrix inversion. A further advantage of this method, as we previously mentioned, is that the impedance matrices computed at each level can be reused for different models that have the same structure beneath that layer.

MODEL RESPONSES

We compare the computed responses from our algorithm with those from the integral equation algorithm of Wannamaker (1991). The integral equation approach was originally outlined in Wannamaker et al. (1984a) and the recent modifications are described in Wannamaker (1991). The model we have chosen for our comparisons is one proposed by Dr. M. S. Zhdanov of the USSR Academy of Sciences in his effort to compile 2-D and 3-D model responses by investigators worldwide. In this section we are striving merely to compare responses from different modeling algorithms, and we are not intending to explore in detail the 3-D responses for complicated geometries. There are several studies that have concentrated on examining 3-D field behavior (Park et al., 1983; Wannamaker et al., 1984b: Park, 1985).

The model under study consists of two adjacent rectangular blocks residing in a three-layer host (see Figure 2). One block is conductive (1 $\Omega \cdot$ m) and the adjacent block is more resistive (100 $\Omega \cdot$ m). The rectangular blocks are imbedded in

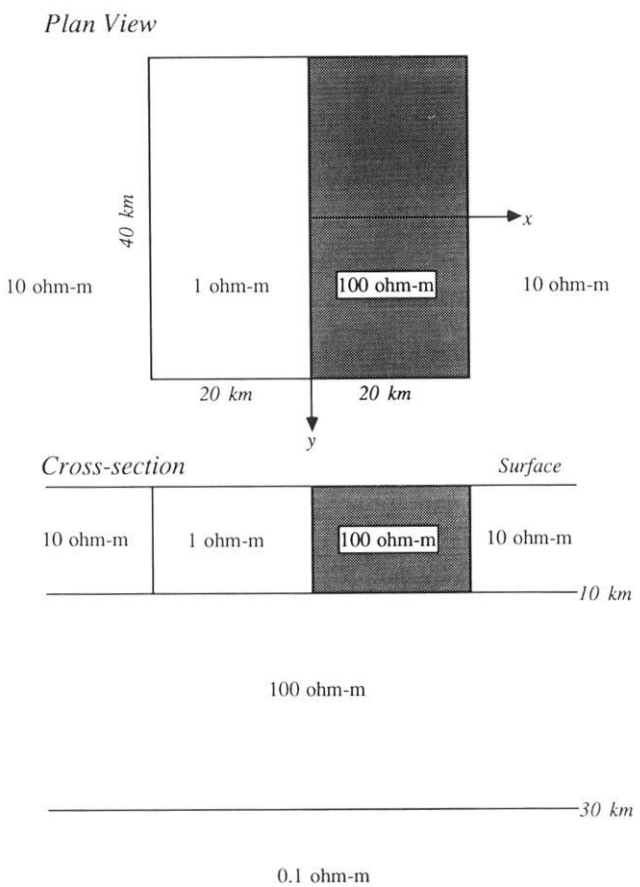

FIG. 2. The 3-D model used to make comparisons between our difference equation algorithms and Wannamaker's (1991) integral equation algorithm.

a layer of 10 Ω . m and are each 20 km in width, 40 km in length, and 10 km in depth. The first layer is underlain by a second layer of 100 Ω l m and 20 km thickness. This layer is then underlain by a half-space of resistivity 0.1 Ω l m. The responses were computed for periods of 10, 100, and 1000 s. The skin depths in the conductive block are 1.6 km, 5 km, and 16 km, respectively and 16 km, 50 km, and 160 km for the resistive block. We define the strike length to be the length of the conductive and resistive bodies in the y-direction. Therefore, the strike length is 40 km for all calculations except when we compare the 3-D results with 2-D results, for which case the strike length is increased to 200 km. For reference, in Figure 3 we show the 1-D response for the three-layer media in which the 3-D bodies reside.

COMPARISONS WITH WANNAMAKER'S SOLUTIONS

The model described above was discretized into 28 blocks in the x-direction, 19 blocks in the y-direction, and 18 layers in the z-direction (11 earth layers and 7 air layers). The model was more finely discretized near the conductivity contrasts (see Figure 4). We will show the apparent resistivities and phases for the Z_{xy} and Z_{yx} responses for profiles across the 3-D body. The Z_{xy} component of the surface impedance tensor is the E_x field due to an applied H_y field.

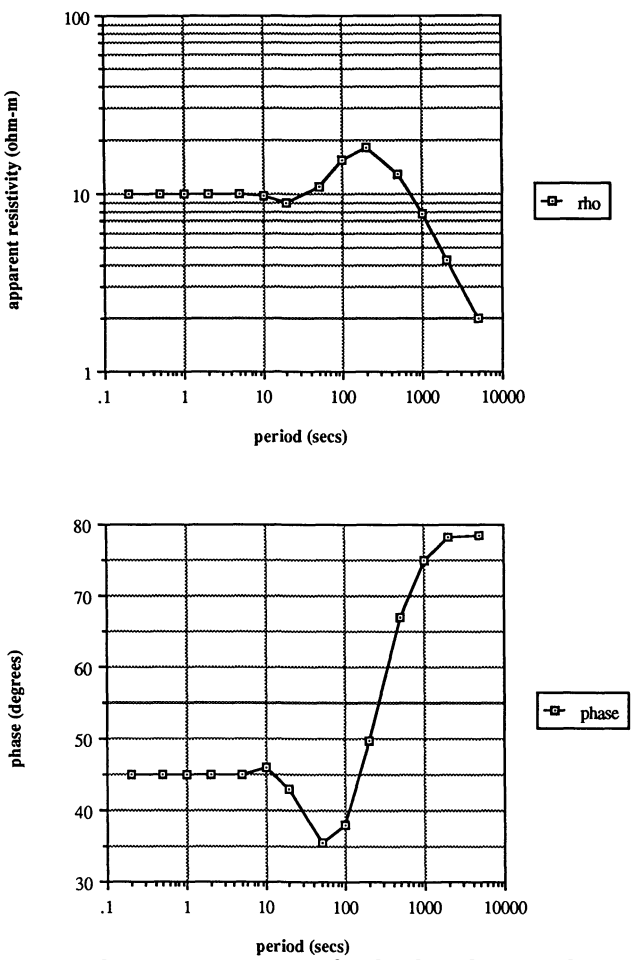

FIG. 3. The 1-D MT response for the three-layer media (see Figure 2) in which the three-dimensional bodies reside.

Similarly, the Z_{yx} component of the surface impedance tensor is the E_y field due to an applied H_x field.

Shown in Figures 5 and 6 are the Z_{xy} mode and Z_{yx} mode responses for the model at a 10-s period for a profile across the center of the bodies (along the x-axis of Figure 2). There is generally good agreement between Wannamaker's responses (labeled as ***rhoxy.ie, phxy.ie,*** etc., where the ***.ie*** stands for integral equation) and our difference equation responses (labeled ***rhoxy.dir, phxy.dir,*** etc. where the ***.dir*** stands for the direct difference equation solution). There are small discrepancies in the phases over the center of the more resistive body and near conductivity contrasts. The phase differences near the boundaries are probably due to a combination of differences in the E field geometry between our difference equation approach and Wannamaker's integral equation approach and differences in the model discretization. The E fields in our algorithm actually represent averages across block faces, whereas in Wannamaker's algorithm, the E fields represent averages for a block and not across block faces. Near conductivity contrasts the E fields are changing rapidly, and the issue is how the E field is averaged to obtain a value that is called the field at a particular location. Finer discretization can be used to obtain more accurate results in areas where strong gradients in the E field exist. (We should point out, however, that field measurements use finite lengths of wire to obtain a measured E value, so only average E values are actually seen.) The difference equation responses were computed with a different model discretization than was used by Wannamaker for the integral equation solutions. In fact, our discretization was somewhat finer near the conductivity contrasts than that used by Wannamaker. We are not certain why there is more phase discrepancy over the center of the resistive body, but

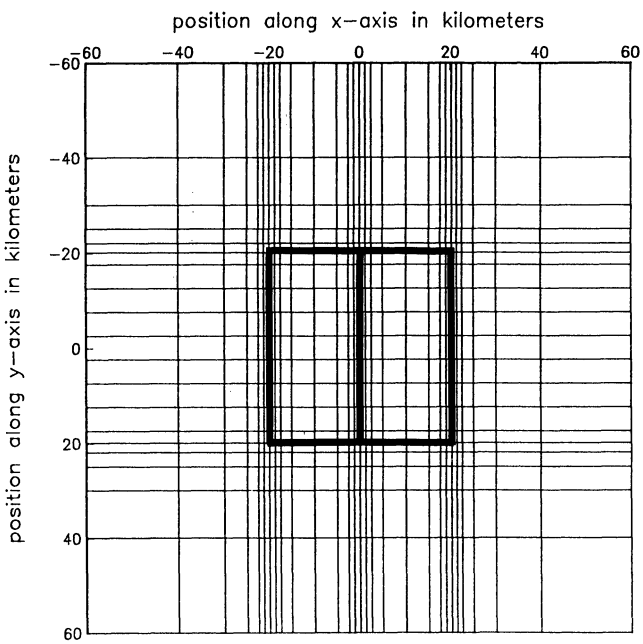

FIG. 4. A plan view of the horizontal discretization used for the model of Figure 2. The model has been more finely discretized near the conductivity contrasts to obtain more accurate solutions in these areas.

it is possible that this may be related to the discretization of the model used in the integral equation solution (Wannamaker, 1990, pers. comm.). Figures 7 and 8 show that the difference equation Z_{xy} and Z_{xy} mode responses at this period agree almost exactly with 2-D transverse magnetic and transverse electromagnetic (TM and TE) mode responses when the strike length of the 3-D body is increased from 40 km to 200 km (effectively making the response across the center of the body a 2-D response since the ends of the 3-D body are many skin depths away from the center).

The Z_{xy} and Z_{xy} mode responses for the model at a 100-s period are shown in Figures 9 and 10, respectively, and the Z_{xy} and Z_{xy} mode responses at a 1000-s period are shown in Figures 11 and 12, respectively. There is excellent overall agreement between Wannamaker's integral equation responses and our difference equation responses, especially in the amplitudes. Discrepancies in phase are usually no more than l-2 degrees and occur primarily near conductivity contacts and over the more resistive body, as before.

We have made additional comparisons at a period of 10 s but for profiles along the strike direction of the bodies (the y-direction as shown in Figure 2). Figures 13 and 14 show the Z_{xy} and Z_{xy} mode responses, respectively as a function of position along the y-axis at a strike position of x = - 10 km (this is down the strike of the conductive body). Likewise, Figures 15 and 16 show the Z_{xy} and Z_{xy} mode responses, respectively as a function of position along the y-axis but at a strike position of x = + 10 km (this is down the strike of the resistive body). As before, there is excellent overall agreement between the integral equation responses and the difference equation responses. Minor phase differences can be found near conductivity contrasts and over the resistive body, and most likely result for the same reasons as stated earlier.

Finally, we compare the vertical magnetic transfer function M_{zx} for the model at a period of 10 s. Figure 17 shows the real and imaginary components of M_{zx} as a function of the position for a profile across the center of the bodies (along the x-axis). Along this profile, M_{zy} is zero due to symmetry. There is excellent agreement between Wannamaker's responses and our difference equation responses. There are small discrepancies in the imaginary component near x = 0 km (this is the interface between the conductive and resistive bodies). This is probably due to a combination of the large gradient in the H_z field near this conductivity boundary and the differences in model discretization.

COMPUTATIONAL CONSIDERATIONS

All of the modeling in this paper was done on the CRAY-2/4-256 computer maintained by the MIT Supercomputer

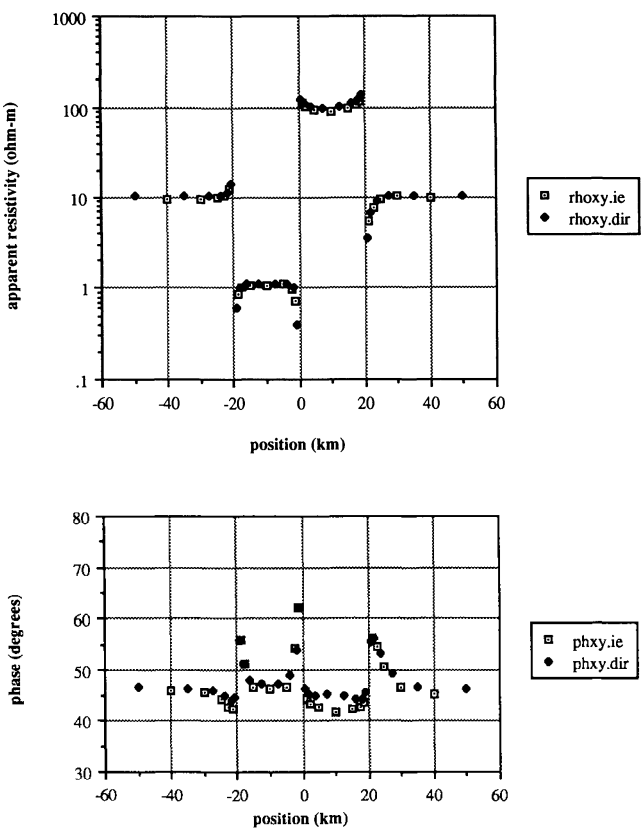

FIG. 5. The Z_{xy} response along a profile across the center of the bodies at a period of 10 s, and a strike length of 40 km (this is the width of the bodies in the y-direction). The responses labeled *rhoxy.ie, phxy.ie,* etc. are those from Wannamaker's (1991) integral equation solution. The responses labeled *rhoxy.dir, phxy.dir,* etc. are those from our direct solution of the difference equations.

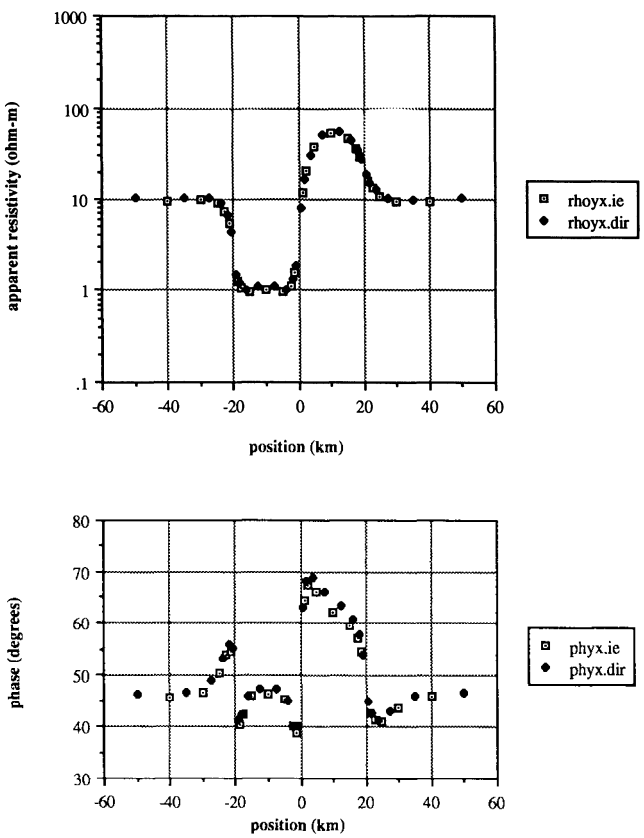

FIG. 6. The Z_{xy} response along a profile across the center of the bodies at a period of 10 s and a strike length of 40 km comparing the integral equation solutions with the direct difference equation solutions.

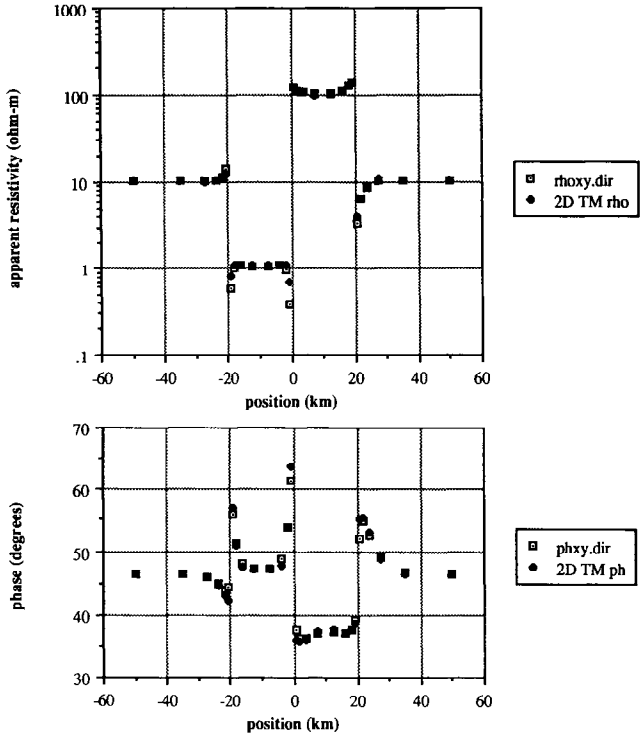

FIG. 7. The Z_{xy} response along a profile across the center of the bodies when the strike length of the bodies is increased to 200 km. The results are for a period of 10 s. Here we are comparing the 3-D difference equation direct solution results along this profile with the 2-D TM results for the profile computed using a 2-D finite-difference (transmission analog) algorithm.

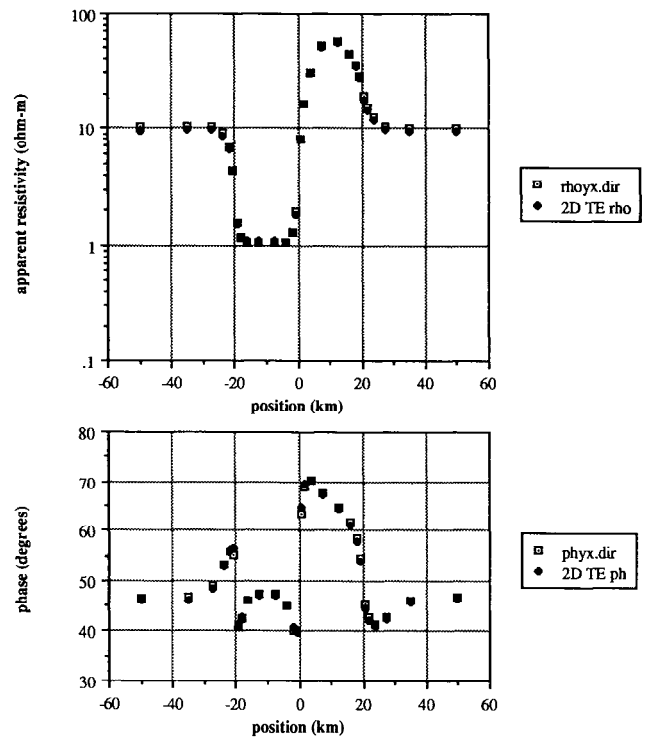

FIG. 8. The Z_{yx} response along a profile across the center of the bodies when the strike length of the bodies is increased to 200 km. The results are for a period of 10 s. Here we are comparing the 3-D difference equation direct solution results along this profile with the 2-D TE results for the profile computed using a 2-D finite-difference (transmission analog) algorithm.

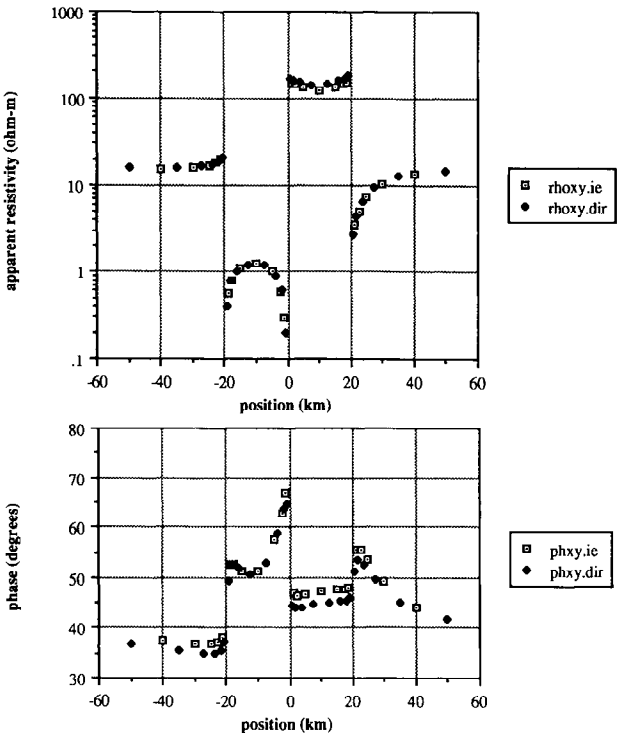

FIG. 9. The Z_{xy} response along a profile across the center of the bodies at a period of 100 s comparing the integral equation solutions with the direct difference equation solutions.

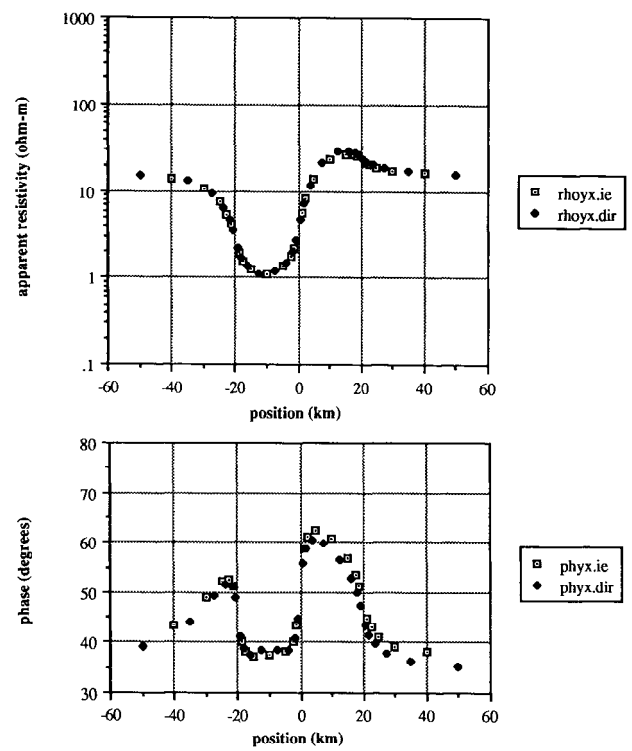

FIG. 10. The Z_{yx} response along a profile across the center of the bodies at a period of 100 s comparing the integral equation solutions with the direct difference equation solutions.

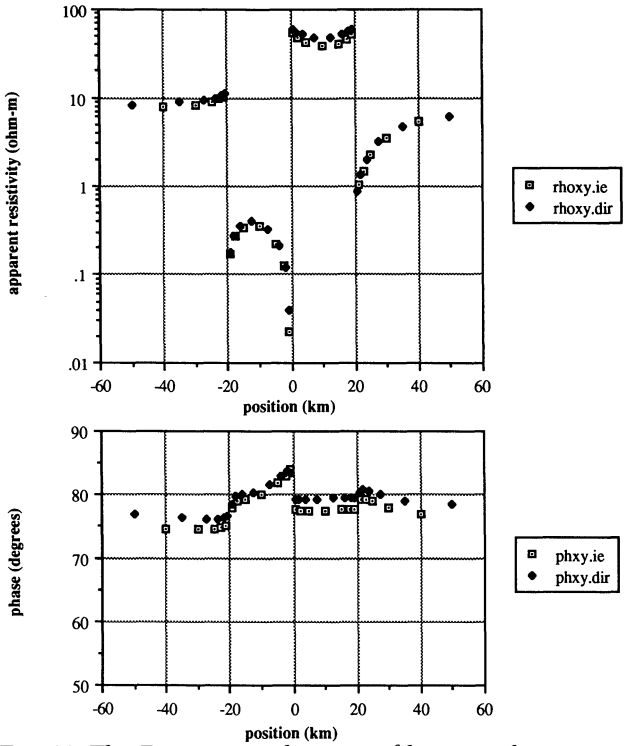

FIG. 11. The Z_{xy} response along a profile across the center of the bodies at a period of 1000 s comparing the integral equation solutions with the direct difference equation solutions.

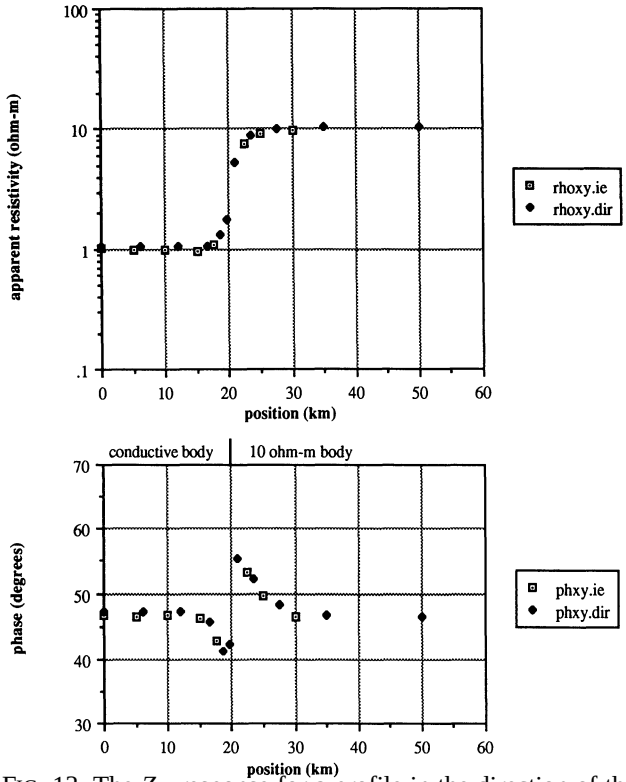

FIG. 13. The Z_{xy} response for a profile in the direction of the y-axis at the position x = -10 km (this is down the strike of the conductive body) and a period of 10 s comparing the integral equation solutions with the direct difference equation solutions.

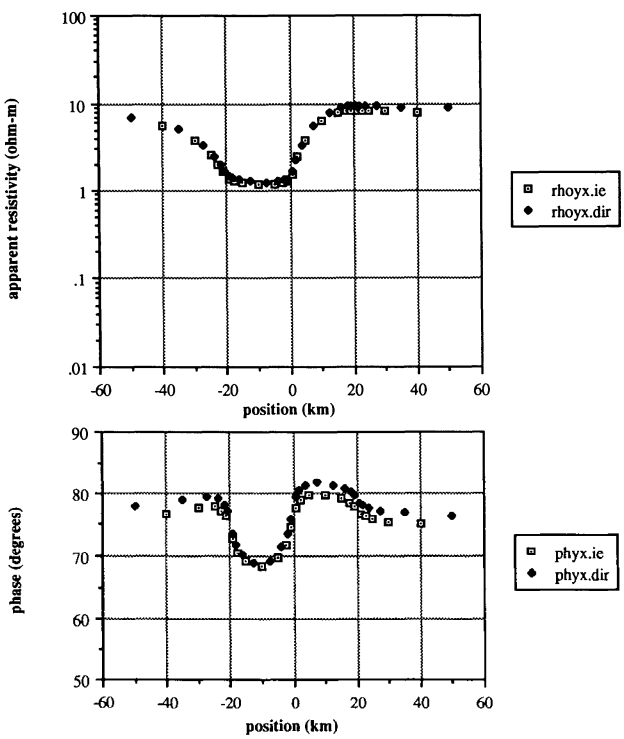

FIG. 12. The Z_{yx} response along a profile across the center of the bodies at a period of 1000 s comparing the integral equation solutions with the direct difference equation solutions.

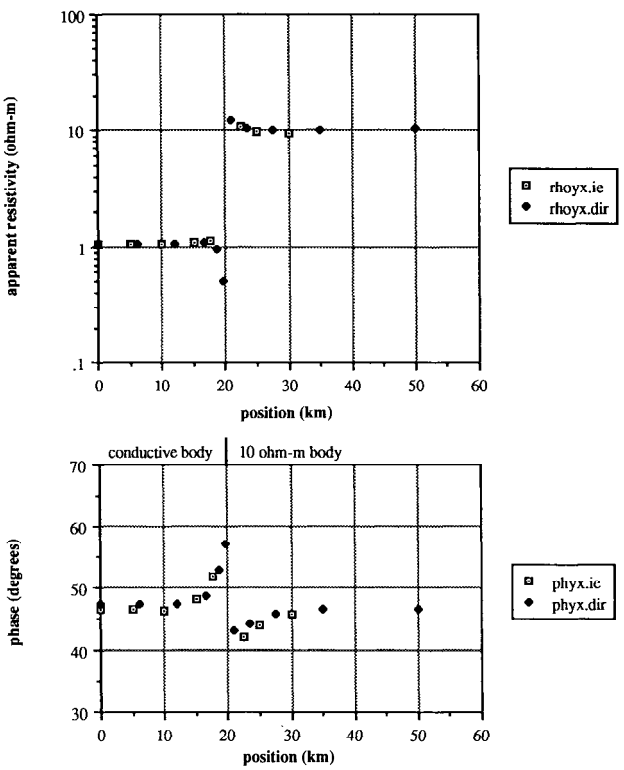

FIG. 14. The Z_{yx} response for a profile in the direction of the y-axis at the position x = -10 km (this is down the strike of the conductive body) and a period of 10 s comparing the integral equation solutions with the direct difference equation solutions.

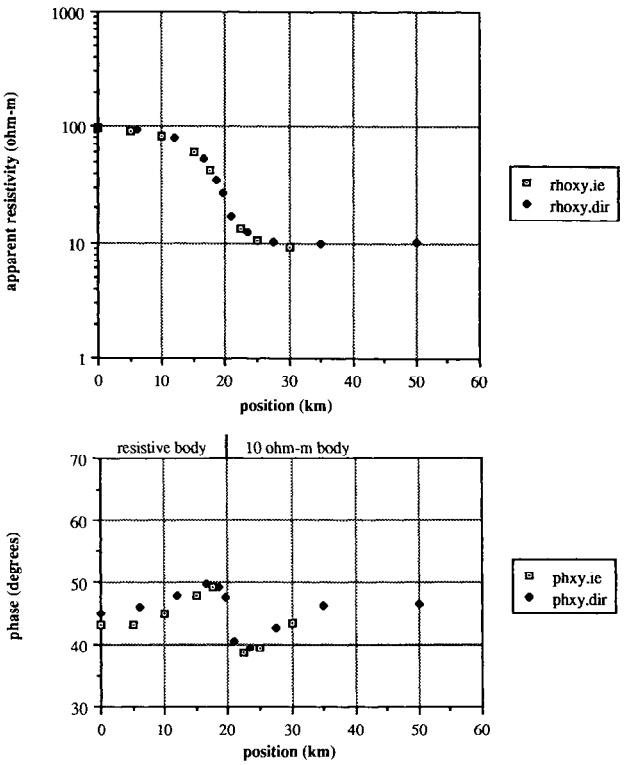

FIG. 15. The Z_{xy} response for a profile in the direction of the y-axis at the position $x = +10$ km (this is down the strike of the resistive body) and a period of 10 s comparing the integral equation solutions with the direct difference equation solutions.

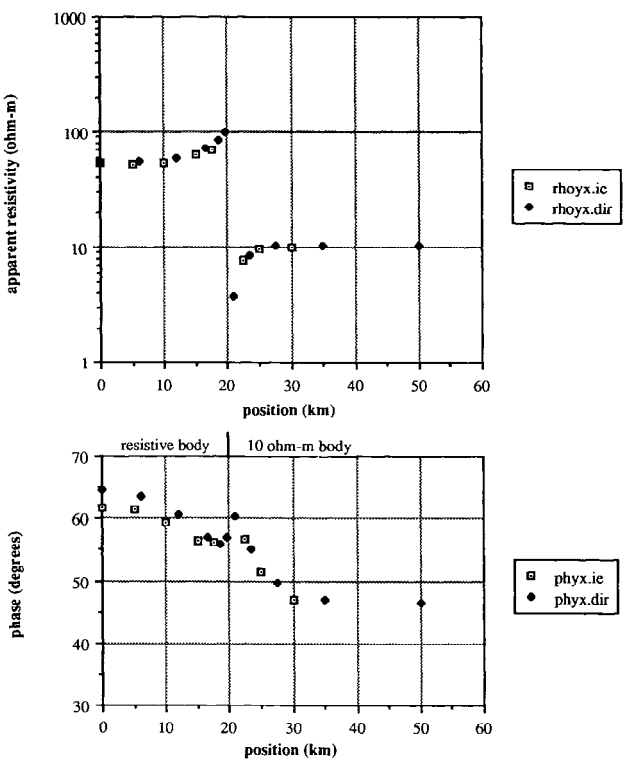

FIG. 16. The Z_{yx} response for a profile in the direction of the y-axis at the position $x = +10$ km (this is down the strike of the resistive body) and a period of 10 s comparing the integral equation solutions with the direct difference equation solutions.

Facility. The Lanczos (1961) method for inverting complex matrices was used in conjunction with CRAY-optimized real matrix inversion routines to invert the complex operators. Additional time-savings were obtained by using the Lanczos (1961) matrix partitioning method for inverting matrices, and by using CRAY-optimized routines for multiplying matrices. It took approximately 25 minutes of CPU time per frequency (two polarizations per frequency) for the direct calculations and 30 MWords of memory (1 word = 8 bytes). This is about the same time and memory used by the integral equation program of Wannamaker (1991) for the same model. For a given model discretization, the complexity of the conductivity model does influence the computation time for the integral equation approach but not for the difference equation approach. Iterative methods can be much quicker, but there are questions about the accuracy of the results.

CONCLUSIONS

We have developed an impedance propagator algorithm to solve for the magnetotelluric response of a 3-D earth model using finite differences on a staggered grid. The finite-difference equations are first-order equations that are based on the integral forms of Maxwell's equations, so the main issue is that of taking averages rather than in approximating derivatives of the fields or earth properties. The results of our algorithm compare favorably with those from Wannamaker's (1991) integral equation solutions for the same model. Minor discrepancies were usually found near conductivity contrasts and over the more resistive body. The

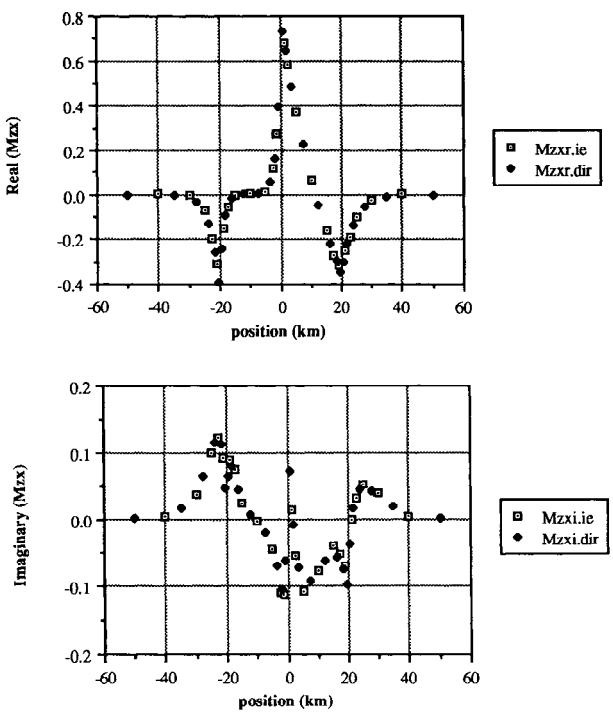

FIG. 17. The real and imaginary components of the M_{zx} response for a profile across the center of the bodies (along the x-axis) for a period of 10 s comparing the integral equation solutions with the direct difference equation solutions.

differences were most likely due to differences in the E field geometry between the two solution algorithms and to different model discretizations.

ACKNOWLEDGMENTS

This work was supported in large part by an industrial consortium of oil companies: Amoco, Chevron, Standard Oil Production Co., Sun, and Texaco. Comments from two anonymous reviewers and Michael Oristaglio greatly improved the manuscript.

REFERENCES

Adhidjaja, J. I., and Hohmann, G. W., 1989, A finite-difference algorithm for the transient electromagnetic response of a three-dimensional body: Geophys. J. Int., 98, 233-242.

Brewitt-Taylor, C. R., and Weaver, J. T., 1976, On the finite-difference solution of two-dimensional induction problems: Geophys. J. Roy. Astr. Soc., 47, 375-396.

Eckhardt, D. H., 1963, Geomagnetic induction in a concentrically stratified earth: J. Geophys. Res., 68, 6273-6278.

Hibbs, R. D., and Jones, F. W., 1976, The calculation of perturbation and induction arrows for a three-dimensional conductivity model and dipole source fields: Pageoph, 114, 997-1008.

Hohmann, G. W., 1975, Three-dimensional-induced polarization and electromagnetic modeling: Geophysics, 40, 309-324.

Jiracek, G. R., Reddig, R. P., and Kojima, R. K., 1989, Application of the Rayleigh-FFT technique to magnetotelluric modeling and correction: Phys. Earth Planet Int., 53, 365-375.

Jones, F. W., 1974, The perturbation of geomagnetic fields by two-dimensional and three-dimensional conductivity inhomogeneities: Pageoph, 112, 793-800.

Jones, F. W., and Pascoe, L. J., 1972, The perturbation of alternating geomagnetic fields by three-dimensional conductivity inhomogeneities: Geophys. J. Roy. Astr. Soc., 27, 479-485.

Lanczos, C., 1961, Linear differential operators: D. Van Nostrand co.

Lines, L. R., and Jones, F. W., 1973a, The perturbation of alternating geomagnetic fields by an island near a coastline: Can. J. Earth Sci., 10, 510-518.

- 1973b, The perturbation of alternating geomagnetic fields by three-dimensional island structures: Geophys . J. Roy. Astr . Soc., 32, 133-154.

Mackie, R. L., 1991, Three-dimensional magnetotelluric modeling and inversion with applications to the California Basin and Range province: Ph.D. thesis, Mass. Inst. of Tech.

Madden, T. R., and Mackie, R. L., 1989, Three-dimensional magnetotelluric modeling and inversion: Proc. IEEE, 77, 318-333.

Morgan, M. A., editor, 1990, Finite element and finite difference methods in electromagnetic scattering: Elsevier.

Park, S. K., 1983, Three-dimensional magnetotelluric modeling and inversion: Ph.D. thesis, Mass. Inst. of Tech.

——— 1985, Distortion of magnetotelluric sounding curves by three-dimensional structures: Geophysics, 50, 785-797.

Park, S. K., Orange, A. S., and Madden, T. R., 1983, Effects of three-dimensional structure on magnetotelluric sounding curves: Geophysics, 48, 1402-1405.

Ranganayaki, R. P., and Madden, T. R., 1980, Generalized thin sheet analysis in magnetotellurics, an extension of Price's analysis: Geophys. J. Roy. Astr. Soc., 60, 445-457.

Reddy, I. K., Rankin, D., and Phillips, R. J., 1977, Three-dimensional modeling in magnetotelluric and magnetic variational sounding: Geophys. J. Roy. Astr. Soc., 51, 313-325.

San Filipo, W. A., and Hohmann, G. W., 1985, Integral equation solution for the transient electromagnetic response of a three-dimensional body in a conductive half-space: Geophysics, 50, 798-809.

Sarkar, T. K., Ed., 1991, Application of conjugate gradient method to electromagnetics and signal analysis: Elsevier Science Publ. Co., Inc.

Stratton, J. A., 1941, Electromagnetic Theory: McGraw-Hill Book co.

Taflove, A., 1988, Review of the formulation and applications of the finite-difference time-domain method for numerical modeling of electromagnetic wave interactions with arbitrary structures: Wave Motion, 10, 547-582.

Taflove, A., and Umashankar, K. R., 1990, The finite-difference time-domain method for numerical modeling of electromagnetic wave interactions with arbitrary structures, in Morgan, M. A., Ed., Finite-element and finite-difference methods in electromagnetic scattering: Elsevier Science Publ. Co., Inc. 287-373.

Wannamaker, P. E., 1991, Advances in three-dimensional magnetotelluric modeling using integral equations: Geophysics, 56, 1716-1728.

Wannamaker, P. E., Hohmann, G. W., and San Filipo, W. A., 1984a, Electromagnetic modeling of three-dimensional bodies in layered earths using integral equations: Geophysics, 49, 60-74.

Wannamaker, P. E., Hohmann, G. W., and Ward, S. H., 1984b, Magnetotelluric responses of three-dimensional bodies in layered earths: Geophysics, 49, 1517-1533.

Weidelt , P., 1975, Electromagnetic induction in three-dimensional structures: J. Geophys., 41, 85-109.

Xinghua, P., Agarwal, A. K., Weaver, J. T., 1991, A theoretical investigation of anisotropic geoelectric structures using three-dimensional numerical models: XX General Assembly, IUGG, Vienna, Austria, IAGA Program and Abstracts, paper GAM 1.6.

Yee, K. S., 1966, Numerical solution of initial boundary value problems involving Maxwell's equations in isotropic media: IEEE Trans. Ant. Prop., AP-14, 302-307.

Zhdanov, M. S., Golubev, N. G., Spichak, V. V., and Varentsov, I. M., 1982, The construction of effective methods for electromagnetic modeling: Geophys. J. Roy. Astr. Soc., 68, 589-607.